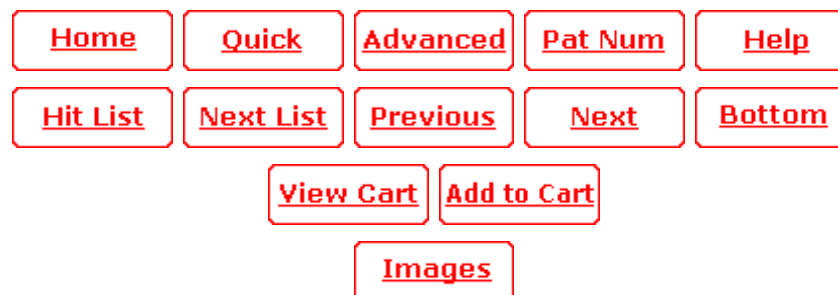


USPTO PATENT FULL-TEXT AND IMAGE DATABASE

(16 of 276)

United States Patent
Zachariah , et al.

7,276,224
October 2, 2007

Synthesis of nanoporous particles

Abstract

Methods of producing nanoporous particles by spray pyrolysis of a precursor composition including a reactive precursor salt and a nonreactive matrix salt are provided, wherein the matrix salt is used as a templating medium. Nanoporous aluminum oxide particles produced by the methods are also provided.

Inventors: **Zachariah; Michael R.** (Eden Prairie, MN), **Liu; Benjamin Y. H.** (North Oaks, MN)

Assignee: **Regents of the University of Minnesota** (Minneapolis, MN)

Appl. No.: **10/167,346**

Filed: **June 11, 2002**

Current U.S. Class: **423/592.1** ; 423/508; 423/593.1; 423/594.17; 423/594.19;
423/604; 423/605; 423/606; 423/608; 423/617; 423/618;

423/624; 423/625; 423/632

Current International Class: C01F 7/00 (20060101); C01B 13/00 (20060101)

Field of Search: 423/22,111,625,21.1,263,592.1,593.1,624,618,617,508,604-608,632,594.17,594.19

References Cited [\[Referenced By\]](#)

U.S. Patent Documents

4138336	February 1979	Mendel et al.
5015373	May 1991	Carr et al.
5108597	April 1992	Funkenbusch et al.
5141634	August 1992	Carr et al.
5182016	January 1993	Funkenbusch et al.
5205929	April 1993	Carr et al.
5254262	October 1993	Funkenbusch et al.
5271833	December 1993	Funkenbusch et al.
5346619	September 1994	Funkenbusch et al.
RE34910	April 1995	Funkenbusch et al.
5540834	July 1996	Carr et al.
5599511	February 1997	Helble et al.
5614472	March 1997	Riddle et al.
5837826	November 1998	Flickinger et al.
5958361	September 1999	Laine et al.
6036861	March 2000	Flickinger et al.

Foreign Patent Documents

0 331 283	Sep., 1989	EP
63-260822	Oct., 1988	JP

S63-260822

Oct., 1988

JP

10-2001-0038293

May., 2001

KR

Other References

- Translation of Korea 10-2001-0038293, May 15, 2001. cited by examiner .
- Dubois., "Preparation of Fine, Spherical Ytria-Stabilized Zirconia by the Spray-Pyrolysis Method," J. Am. Ceram. Soc., 1989; 72(4):713-15. cited by other .
- Efendiev et al., "A model for two-component aerosol coagulation and phase separation: a method for changing the growth rate of nanoparticles." Chemical Engineering Science, 2001: 56:5763-5769. cited by other .
- Ehrman et al., "Effect of temperature and vapor-phase encapsulation on particle growth and morphology," J. Mater. Res., Apr. 1999; 14(4):1664-1671. cited by other .
- Fan et al., "Multiphased assembly of nanoporous silica particles," J. Non-Crystalline Solids, 2001; 285:71-8. cited by other .
- Fissan et al., "Determination of Particle Size Distributions By Means of an Electrostatic Classifier," J. Aerosol Sci., 1983; 14:354-357. cited by other .
- Gadalla et al., "Preparation of fine, hollow, spherical NiFe.sub.2O.sub.4 powders," J. Mater. Res., Dec. 1990; 5(12):2923-7. cited by other .
- Goltner et al., "Mesoporous Materials by Templating of Liquid Crystalline Phases," Adv. Mater., 1997; 9(5):431-436. cited by other .
- Guinier, X-Ray Diffraction in Crystals, Imperfect Crystals, and Amorphous Bodies, Freeman, San Francisco, 1963, title page, publication page, and p. 124. cited by other .
- Holland et al., "Synthesis of Macroporous Minerals with Highly Ordered Three-Dimensional Arrays of Spheroidal Voids," Science, Jul. 24, 1998; 281 :538-540. cited by other .
- Iskandar et al., "In Situ Production of Spherical Silica Particles Containing Self-Organized Mesopores," Nano Letters, 2001; 1 (5):231-234. cited by other .
- Kim et al., "Synthesis of Nanoporous Metal Oxide Particles by a New Inorganic Matrix Spray Pyrolysis Method," Chem. Mater., Jun. 17, 2002; 14(7):2889-99: published on Web Jun. 17,

2002. cited by other .

Knutson et al., "Accurate measurement of aerosol electric mobility moments," J. Aerosol Sci., 1975; 6:453-460. cited by other .

Kodas et al., Aerosol Processing of Materials, Wiley-VCH, 1999, title page, publication page and table of contents only, 14 pages. cited by other .

Kodas et al., "Alumina Powder Production by Aerosol Processes," Alumina Chemicals: Science and Technology Handbook, The American Ceramic Society, Inc., 1990, title page, publication page and pp. 375-383. cited by other .

May, "The Collision Nebulizer. Description, Performance and Application." J. Aerosol Sci., 1973; 4(3):235-243. cited by other .

Seinfeld et al., Atmospheric Chemistry and Physics from Air Pollution to *Climate Change*, John Wiley & Sons, Inc., 1998, title page, publication page and table of contents only, 19 pages. cited by other .

Senzaki et al., "Preparation of Strontium Ferrite Particles by Spray Pyrolysis," J. Am. Ceram. Soc., 1995; 78(11):2973-6. cited by other .

Struchtrup et al., "A model for kinetically controlled internal phase segregation during aerosol coagulation," J. Aerosol Sci., 2001; 32:1479-1504. cited by other .

Velev et al., "Microstructured porous silica obtained via colloidal crystal templates," Chem. Mater., 1998; 10:3597-3602. cited by other .

Xia et al., "Synthesis of CeO₂ nanoparticles by salt-assisted ultrasonic aerosol decomposition," J. Mater. Chem., 2001; 11:2925-2927. cited by other .

Xia et al., "Novel Route to Nanoparticle Synthesis by Salt-Assisted Aerosol Decomposition," Adv. Mater., 2001; 13(20):1579-1582. cited by other .

Zachariah et al., "Aerosol processing of YBaCuO superconductors in a flame reactor," J. Mater. Res., Feb. 1991; 6:264-9. cited by other .

Ciminelli, "Synthesis of Alumina From Al(NO₃)₃·9H₂O by the Evaporative Decomposition of Solution Process," Master of Science Thesis, 1983, Pennsylvania State University. cited by other .

Weast, Ed., Handbook of Chemistry and Physics, 55th Ed., Cleveland, OH, 1974, cover page, title page, pp. B-122 & B-137. cited by other .

Windholz et al, Eds., The Merck Index, Rahway, NJ, 1983, cover page, title page, p. 140. cited by other.

Primary Examiner: Bos; Steven

Attorney, Agent or Firm: Mueting Raasch & Gebhardt, P.A.

Claims

What is claimed is:

1. A method of forming nanoporous particles comprising a metal oxide, the method comprising: providing a precursor composition comprising at least one reactive precursor salt and at least one matrix salt, wherein the decomposition temperature of the reactive precursor salt is lower than the melting point of the matrix salt; spray pyrolyzing the precursor composition, thereby forming precursor droplets, at a temperature below the melting point of the matrix salt and above the decomposition temperature of the precursor salt to form particles comprising matrix salt and decomposed precursor salt, wherein the relative humidity of spray pyrolyzing is carried out at a relative humidity of at least about 50% and no greater than about 80%; and rinsing the matrix salt from the particles to form nanoporous metal oxide particles.
2. The method of claim 1 wherein the precursor composition comprises a mole ratio of precursor salt to matrix salt of at least about 1:1 and no greater than about 1:5.
3. The method of claim 2 wherein the precursor composition comprises a mole ratio of precursor salt to matrix salt that is no greater than about 1:3.
4. The method of claim 1 wherein the total concentration of precursor salt and matrix salt in the precursor composition is at least about 1 weight percent and no greater than about 3 weight percent, based on the total weight of the precursor composition.

5. The method of claim 1 wherein the spray pyrolyzing is carried out at a temperature of at least about 200.degree. C. and no greater than about 700.degree. C.
6. The method of claim 5 wherein spray pyrolyzing is carried out at a temperature no greater than about 550.degree. C.
7. The method of claim 1 wherein the precursor composition is spray pyrolyzed under conditions effective to form particles and allow the matrix salt to diffuse into the interior of the particles.
8. The method of claim 1 wherein the diameter of the nanoporous metal oxide particles is at least about 90 nanometers.
9. The method of claim 1 wherein the precursor salt is selected from the group consisting of Group IIIA metal salts, Group IVA metal salts, Group VA metal salts, Group VIA metal salts, transition metal salts, and combinations thereof.
10. The method of claim 1 wherein the matrix salt is selected from the group consisting of fluorides, chlorides, bromides, iodides, and combinations thereof.
11. The method of claim 1 wherein the precursor composition is an aqueous precursor composition.
12. The method of claim 1 wherein rinsing comprises rinsing in an aqueous rinse to provide nanoporous metal oxide particles.
13. The method of claim 1 wherein the nanoporous metal oxide particles have a pore size of at least about 2 nanometers and no greater than about 20 nanometers in diameter.
14. The method of claim 9 wherein the precursor salt is selected from the group consisting of Group IIIA metal salts, Group IVA metal salts, Group VA metal salts, and combinations thereof.

the aluminum salt to form particles comprising alkali metal salt and decomposed aluminum salt, wherein the precursor composition is spray pyrolyzed under conditions to form aluminum oxide; and rinsing the alkali metal salt from the particles of alkali metal salt and decomposed aluminum salt in an aqueous rinse to form nanoporous particles of aluminum oxide.

23. The method of claim 22 wherein the nanoporous aluminum oxide particles have a pore size of at least about 2 nanometers and no greater than about 20 nanometers in diameter.

24. The method of claim 22 wherein the aluminum salt is aluminum nitrate.

25. The method of claim 22 wherein the alkali metal salt is sodium chloride.

Description

BACKGROUND

Microporous inorganic solids, such as synthetic and naturally-occurring zeolites, have found wide use in such applications as molecular sieves, filtration, and purification materials, due to their large internal surface area. However, because of the limitation of pore size of these materials to typically no smaller than about 1.5 nanometers (nm), new synthetic methods have been investigated to extend the range of available pore sizes of porous inorganic materials, such as metal oxides. Such methods include using templates of surfactant liquid (Goltner et al., *Adv. Mater.*, 9(5):431 (1997)) and colloidal (Velev et al., *Chem. Mater.*, 10:3597 (1998)) crystals to produce mesoporous materials with pore diameters of about 2 nm to about 10 nm. These new methods successfully expand the porosity of zeolite-type materials. However, although these methods provide useful materials for expanded opportunities in the fields of molecular sieving and chemical adsorption, these methods have the disadvantage of requiring a secondary hydrothermal process to remove the surfactant. Such thermal processes may result in collapse of the porous structure.

Furthermore, most templating procedures in batch reactor operations require time-consuming methods, one-time-only use of the templating material, and auxiliary solvent extraction. Such considerations may

make otherwise promising applications using the porous materials commercially uneconomical.

Nanoporous alumina is a preferred product because it is increasingly being used in adsorption and catalysis, wherein their large surface area, pore structure, and unique surface chemistry play essential roles (Kodas et al., "Alumina Powder Production by Aerosol Processes," Alumina Chemicals: Science and Technology Handbook, The American Ceramic Society, Inc. (1990)).

Metal and metal oxides may be useful as a porous inorganic material in such applications as previously described, provided an adequate porosity is achieved. Metal and metal oxide particles may be easily produced by the spray pyrolysis process, which is one of the simplest and most industrially viable production methods in use. Spray pyrolysis involves the use of one or more precursors dissolved in a solvent and aerosolized into a droplet stream, which is then typically processed in a tubular reactor or flame (Zachariah et al., *J. Mat. Res.*, 6:264(1991)). Typically, solvent evaporation is accompanied by precursor precipitation, and a thermally driven reaction to produce the final product. A wide variety of materials have been produced by this method using single and multi-component metals and metal-oxides (Kodas et al., *Aerosol Processing of Materials*, Wiley-VCH (1999)). A well known approach using spray pyrolysis to produce metal oxides involves using metal nitrate salts, which are readily available, have reasonable solubility in water, and decompose at moderate temperatures (less than about 500.degree. C.). Conventional spray pyrolysis processes may, however, provide hollow particles of metal oxides (Dubois et al., *J. Am. Ceram. Soc.*, 72(4):713 (1989); Gadalla et al., *J. Mater. Res.*, 5(12):2923 (1990); Senzaki et al., *J. Am. Ceram. Soc.*, 78(11):2973 (1995)) which may not provide sufficient particle surface area for an intended application. There is a need, therefore, for a spray pyrolysis process that provides a nanoporous metal oxide material that is able to provide adequate particle surface area for an intended application.

Recently, mesoporous silica particles have been produced by a spray pyrolysis method, in which polystyrene spheres and surfactants are employed to produce multiphased self-assembly nanostructures in an evaporating droplet mixed with tetraethylorthosilicate (TEOS, $\text{Si}(\text{OCH}_2\text{CH}_3)_4$), ethanol, and water (Fan et al., *J. Non-Crystalline Solids*, 285:71 (2001)). However, this process has the disadvantage of requiring a secondary thermal calcination process to remove the nanophased additives from the matrix of the silica/surfactant/polystyrene spheres that, as indicated above, may cause a collapse

nanoporous particles. Alternatively, the precursor composition may be spray pyrolyzed under conditions effective to provide metal oxide nanoporous particles.

To provide the preferred nanoporous particles of the invention, it is important that the precursor salt and the matrix salt are chosen such that the precursor salt decomposes at a temperature below the melting point of the matrix salt. Suitable precursor salts and matrix salts are also capable of being spray pyrolyzed from a precursor composition. Typical preferred precursor salts of the invention are those that decompose at temperatures from about 200.degree. C. to about 600.degree. C. Additionally, preferred precursor salts typically are more soluble, at room temperature, in the vehicle of the precursor composition than the selected matrix salt of the precursor composition.

Preferred precursor salts of the invention include salts selected from the group of Group IIIA metal salts, Group IVA metal salts, Group VA metal salts, Group VIA metal salts, Group VIIA metal salts, transition metal salts, and combinations thereof. The Group IIIA-Group VIIA metal salts, particularly the Group VIA and Group VIIA metal salts include salts of those elements understood by those skilled in the art to be metalloids. Metalloids show characteristics of both metals and nonmetals, and include silicon, arsenic, tellurium, and antimony. Transition metal salts are metal salts including metals chosen from Group IB, Group IIB, Group IIIB, Group IVB, Group VB, Group VIB, Group VIIB, and Group VIII of the Periodic Table.

Anions useful in preferred precursor salts are those that form a salt with the selected metal to provide a precursor composition of the invention, and that provide the desired metal or metal oxide particle upon spray pyrolysis of the precursor composition. Preferred anions are nitrates, carbonates, and acetates. More preferred anions are nitrates.

More preferred precursor salts include salts selected from the group of Group IIIA metal salts, Group IVA metal salts, Group VA metal salts, and combinations thereof. Even more preferred precursor salts are salts selected from Main Group IIIA metal salts. A particularly preferred precursor salt is aluminum nitrate.

The precursor composition can also include a carrier (i.e., a precursor vehicle), such as water, or any other

$(t_{vd})^{2.02} \cdot 10^{-8}$ Droplet shrinkage $\cdot (t_r)^{1.69} \cdot 10^{-4}$ Solute diffusion $\cdot (t_{sd})^{3.49} \cdot 10^{-4}$ Heat conduction in air $\cdot (t_{hg})^{2.23} \cdot 10^{-7}$ Heat conduction in 3.41 $\cdot 10^{-6}$ droplet $\cdot (t_{hl})^{0.5}$ $t_{vd} = d_p^2 / D_v$, R = droplet radius [cm], D_v = diffusivity of solvent vapor in air [$\text{cm}^2 \cdot \text{s}^{-1}$], where, R is assumed to be 350 nm, which was measured by laser spectrometry $\cdot \rho \cdot \infty$ $\cdot \text{versal constant}$, D_v = diffusion coefficient of water vapor, M = molecular weight of water, p_d = partial pressure of solvent vapors on the droplet, p_∞ = partial pressure of solvent vapors far from the droplet $\cdot (t_{sd})^3 = d_p^2 / D_l$, D_l = diffusivity of solute in liquid phase [$\text{cm}^2 \cdot \text{s}^{-1}$], $(t_{hg})^4 = d_p^2 / \alpha_g$, α_g = thermal diffusivity in the gas phase [$\text{cm}^2 \cdot \text{s}^{-1}$], $(t_{hl})^5 = d_p^2 / \alpha_l$, α_l = thermal diffusivity in the liquid phase [$\text{cm}^2 \cdot \text{s}^{-1}$]

Table 1 shows that salt diffusion and droplet shrinkage, manipulated through, for instance, precursor evaporation rates, are clearly the slowest processes among various mechanisms that occur during spray pyrolysis. Further, they both require sufficiently comparable amounts of time for completion such that a change in process parameters may have an effect on the predominance of one mechanism over the other.

Manipulation of the matrix salt diffusion and precursor evaporation rates may be effected by varying spray pyrolysis conditions. Such conditions include dwell time in the dryer and furnace; the nebulized droplet size; drying conditions, through regulation of relative humidity; and pyrolysis temperature. Matrix salt diffusion and precursor evaporation may also be manipulated through the conditions of the precursor composition, as previously indicated, such as total salt concentration and/or the mole ratio of precursor salt to matrix salt in the precursor composition. Without being bound to any particular theory, it is believed that manipulation of the above pyrolysis conditions and precursor compositions play significant and, particularly, interrelated roles in determining the particles' final nanoporous structure.

Spray Pyrolysis and Characterization of Precursor Compositions

Aluminum oxide particles were produced by the method of Example 1, except that the relative humidity at the dryer outlet was about 65%. The resulting pore surface area and volume distribution is provided in FIGS. 5(a) and 5(b).

Example 3

Aluminum oxide particles were produced by the method of Example 1, except that the relative humidity at the dryer outlet was about 50%. The resulting pore surface area and volume distribution is provided in FIGS. 5(a) and 5(b).

As indicated by Examples 1-3, varying evaporation rates through manipulation of relative humidities had a significant effect on the structure of the resulting particles. FIG. 5 reports the resultant pore volumes and pore surface areas of nanoporous particles produced at various relative humidities. Higher rates of droplet evaporation (at lower relative humidities) are believed to result in particles having larger pore diameters than particles produced at higher relative humidities. However, the larger average pore diameters seen at higher droplet evaporation rates occurred typically at the higher end of the pore diameter measurements and were associated with the formation of hollow-like structures. As shown in FIG. 5, there is a trend toward the formation of greater pore volume in the particles having smaller pores (about 2 to about 10 nanometers) with a higher relative humidity (decreased drying rate), indicating that in the preferred methods of the present invention, the precursor composition is spray pyrolyzed at a relative humidity that is preferably at least about 50%, more preferably at least about 65%, and preferably at a relative humidity of no greater than about 80%.

Without being held to any particular theory, it is believed that a certain amount of control of the competition between salt diffusion and precursor composition evaporation is accomplished by a change in relative humidity. In a high relative humidity environment, typically above about 60% relative humidity, at room temperature and pressure, highly porous structured particles are typically produced without the formation of hollow-structured particles due, presumably, to a reduction of crust formation. In FIG. 7, the ratio of the characteristic time of droplet shrinkage ($t_{\text{sub.r}}$) to that of salt diffusion ($t_{\text{sub.sd}}$) within the

Aluminum oxide particles were produced by the method of Example 8, except that the pyrolysis temperature was about 200.degree. C. The resulting pore surface area and volume distribution is provided in FIGS. 8(a) and 8(b).

Example 10

Aluminum oxide particles were produced by the method of Example 8, except that the pyrolysis temperature was about 700.degree. C. The resulting pore surface area and volume distribution is provided in FIGS. 8(a) and 8(b).

Example 11

Aluminum oxide particles were produced by the method of Example 8, except that the pyrolysis temperature was about 400.degree. C. The resulting pore surface area and volume distribution is provided in FIGS. 8(a) and 8(b).

Example 12

Aluminum oxide particles were produced by the method of Example 8, except that the pyrolysis temperature was about 800.degree. C. The resulting pore surface area and volume distribution is provided in FIGS. 8(a) and 8(b).

By the method of Example 8 it is shown that the maximum total surface area under these precursor evaporation conditions and for this precursor composition occurs at a pyrolysis temperature of about 550.degree. C. Further, under the conditions of this Example, nanoporous particles were produced with the greatest proportion of small pore sizes, relative to the other pyrolysis temperatures tested. For the methods of Examples 9, 10, and 11, pyrolyzed at temperatures of about 200.degree. C., about 700.degree. C., and about 400.degree. C., respectively, nanoparticles apparently may have been formed, although there was a decline in small pore volume relative to the nanoporous particles formed at the intermediate temperature of about 550.degree. C. in each case. In the case of the low pyrolysis temperature of Example 9, about

tend to collapse. At the highest temperature recorded (about 800.degree. C., FIG. 8(b)) a substantially total collapse of the porous or hollow nature of the particle is observed, presumably because the matrix salt has substantially melted and, therefore, cannot preserve the porous network.

Conversely, at the lower temperature ranges (below about 400.degree. C.), increasing particle surface area is seen, along with larger pore volumes as compared with pore volumes produced in particles pyrolyzed at the intermediate temperatures, such as about 400.degree. C. and about 550.degree. C. (FIGS. 8(a) and 8(b)). It is believed that particles formed at the lowest temperature (about 200.degree. C.) having large pores, and the increase in surface area with increasing temperature (for temperatures below about 550.degree. C.) is the result of incomplete decomposition, and subsequent loss, of the precursor salt, as well as matrix salt. Incomplete thermal decomposition of the aluminum nitrate may result in some of the aluminum content being leached with the sodium chloride during the washing process. This presumably results in less particle surface area per unit mass.

While each condition identified above is believed to affect the final particle morphology individually, it is also believed that the conditions are additionally interrelated. For instance, without being held to any particular theory, it is believed that the concentration of salts, especially the concentration of the matrix salt, typically affects the size and porosity of the final particle, in particular when considering the processing temperature and the melting point of the chosen matrix salt. For instance, it is believed that if a precursor composition including a matrix salt fraction that is higher than 3 parts matrix salt to 1 part precursor salt is spray pyrolyzed at intermediate temperatures that are generally below the deposition temperature of the precursor salt, the porous structure presumably never forms enough rigidity and can be washed away.

If, on the other hand, the processing takes place at a high temperature (e.g., about 700.degree. C. or greater), above the deposition temperature of the precursor salt and near or above the melting point of the matrix salt, using the same high matrix salt precursor composition, fragments of the metal of the precursor salt may be allowed to nucleate and grow by internal droplet diffusion. These conditions are typically believed to produce, after washing to remove the matrix salt, substantially nonporous nanoparticles (Ehrman et al., J. Mater. Res., 14(4):1664 (1999); Struchtrup et al., J. Aerosol. Sci., 32:1479 (2001);

However, by defocusing the beam so that the particle is imaged at the surface, information about the particle's surface structure can be deduced. In the present invention the porous structures shown in FIG. 10 are apparent. The particles that were produced at the lowest temperature (about 200.degree. C.), after matrix salt removal, showed highly open, broken shell structures, as if the only structures that remained were thin crusts. This is presumably due to a small amount of the nitrate that was converted to the oxide, and significant amounts of the aluminum nitrate that was carried away with the aqueous wash. Additionally, at the highest temperature (about 800.degree. C.), the interpretation was not clear, since at that temperature the pore structure had collapsed.

FIG. 9 shows specific surface area and pore size distributions of nanoporous oxide particles produced by the preferred methods of the present invention and determined by a Gas Sorptometer (BET; ASAP 2000, Micrometrics; nitrogen adsorption at 77K). The precursor composition included about a 1 weight percent total salt concentration, based on total weight of the composition, and about a 1:1 mole ratio of aluminum nitrate to sodium chloride. The precursor composition was spray pyrolyzed at a temperature of about 550.degree. C. and a relative humidity of about 30%. FIG. 9(a) shows specific surface areas of the particle of only a few square meters per gram, with a near monotonic increase in pore volume with increasing pore diameter. The pore volume increase presumably arises from hollow particles that are observed in the SEM, corresponding to a very small surface area.

More interesting is the analysis of particles following aqueous leaching of the Matrix salt (FIG. 9(b)). Pore volume shows a bimodal distribution, with the large mode corresponding to hollow particles and the smaller mode corresponding to the nanoporous structure revealed as a result of removal of the matrix salt.

Powder X-ray diffraction patterns (XRD; Model D-5000, Siemens, using CuK.alpha. radiation) are shown in FIGS. 11(a) and 11(b) for nanoporous aluminum oxide particles produced by spray pyrolysis both prior to (FIG. 11(a)) and after (FIG. 11(b)) aqueous wash. The precursor composition included about a 1 weight percent concentration, based on total weight of the composition, of aluminum nitrate and sodium chloride, with the salts present in the aqueous precursor in a mole ratio of about 1:1. For the resulting nanoporous oxide particles, the spectra showed very strong diffraction from salt with a crystallite size estimated using Scherrer's equation (Guinier, X-Ray Diffraction, Freeman, San Francisco, page 124 (1963)) of about 7

